JOURNAL OF NATURAL PRODUCTS

pubs.acs.org/jnp

Article

Antioxidant Activity of Compounds Isolated from *Elaeagnus umbellata* Promotes Human Gingival Fibroblast Well-Being

Anna Maria Iannuzzi, Chiara Giacomelli, Marinella De Leo, Deborah Pietrobono, Fabiano Camangi, Nunziatina De Tommasi,* Claudia Martini, Maria Letizia Trincavelli, and Alessandra Braca

Cite This: *J. Nat. Prod.* 2020, 83, 626−637

Read Online

ACCESS | Metrics & More | Article Recommendations | Supporting Information

ABSTRACT: Four new triterpenoid bidesmosidic saponins (**1**−**4**) and a sesquiterpenoid glucoside (**5**), together with nine known phenolic compounds (**6**−**14**), were isolated from the fruits of *Elaeagnus umbellata*. Their structures were elucidated using 1D and 2D NMR spectroscopy and mass spectrometry data. The antioxidant capability of the isolated compounds was evaluated in human gingival fibroblasts. Compound **6** decreased ROS production and promoted cell proliferation. It also counteracted the cell cycle blockade induced by a low concentration of H_2O_2 decreasing the expression of p21 and CDKN2A ($p16^{INK4A}$). Compound **6** decreased the expression of inflammatory cytokines (IL-6 and IL-8) in response to inflammatory stimuli, supporting its possible use in periodontitis lesions.

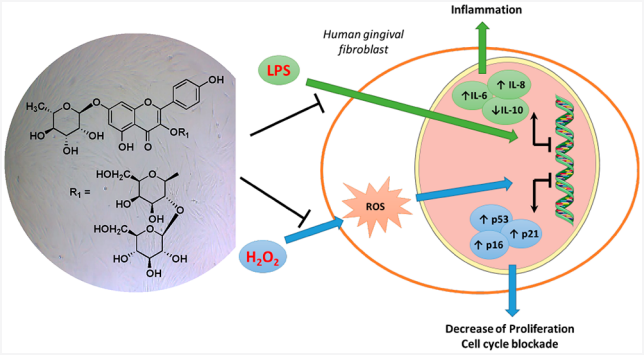

The genus *Elaeagnus* (Elaeagnaceae) includes about 90 species spread around the world, particularly in the temperate and subtropical regions of Asia, most of which are considered as folk medicinal plants for their pharmacological effects.[1] Among these species, *Elaeagnus umbellata* Thunb, also known as "cardinal olive" or "autumn olive", is a small deciduous shrub that grows as a tree 5−6 m tall, native to Southern Europe and Central Asia and then introduced to North America as an ornamental plant.[2] In Indian traditional medicine, *E. umbellata* flowers are used in cardiac and respiratory diseases, while the seed oil is used for the treatment of pulmonary infections, coughs, and cardiac ailments.[3] In Japan and China, the leaves are used as a tonic and their decoction is used to treat bowel disorders.[4] The fruits, produced in great quantities and ripening between September and November, are small, round, juicy, reddish to pink, dotted with scales, and carrying a single seed.[5] The fruits are edible, but not widely cultivated and consumed as a food, except for some areas of Asia, where the fruits are incorporated into the common diet, due to their benefits against hepatitis, fractures, injuries, and diarrhea, and used to prepare juices, jams, preserves, and other food stuffs.[6] The red pigmentation of the berries is due to the presence of a large amount of carotenoids, especially lycopene (about 5−20 times higher than that of the ordinary tomato), which is reported to have anticancer, antioxidant, hepatoprotective, and cardioprotective effects.[5,6] Therefore, these fruits have recently been used for the development of lycopene-rich extracts or powders for food formulation.[5] In Italy, the plant is nonindigenous and is cultivated for ornamental purposes, while the fruits are eaten fresh, a custom that was imported from Asia.[7] Few phytochemical investigations on *E. umbellata* berries are reported describing the presence of bioactive compounds such as polyphenols and flavonoids, which contribute in part to the in vitro antioxidant activity of "cardinal olive" extracts,[2] and also alkaloids, steroids, terpenoids, and saponins.[8]

Thus, the present work was carried out to fully investigate the chemical profile of *E. umbellata* fruits cultivated in Italy, leading to the isolation and structural characterization of five new compounds, including four triterpenoid saponins (**1**−**4**) and one sesquiterpenoid glucoside (**5**), together with nine known phenolics (**6**−**14**). It is well known that flavonoid aglycones and corresponding glycosides possess antioxidant and anti-inflammatory activities.[9−11] Oxidative stress and related inflammatory processes play crucial roles in different pathologies of the oral cavity such as periodontitis and oral mucositis. Periodontitis is a common inflammatory disease that derives from bacterial infection and proceeds with an abnormal host response. It can result in the destruction of oral soft tissues and can affect systemic health.[12] Oral mucositis is one of the most common side effects observed during cancer radiotherapy and chemotherapy treatment.[13] The modulation

Special Issue: Special Issue in Honor of Jon Clardy

Received: October 17, 2019
Published: February 7, 2020

of reactive oxygen species (ROS) has gained attention due to their pivotal role in the progression of oral inflammatory diseases.[14] ROS are a group of molecules derived by the physiological metabolism of oxygen in cells, and intracellular ROS such as hydrogen peroxide (H_2O_2) have been widely investigated for their controversial role. In the host response to bacterial infection, the activation of neutrophils promotes ROS production[15] that causes the damage of different macromolecules, leading to a premature aging of periodontal tissue.[16] Similarly, the production of ROS by radiotherapy and chemotherapy plays a pivotal role in the initiation phase of oral mucositis.[17] Recently, several efforts have been made to discover synthetic molecules, natural extracts, and compounds that could locally counteract the production of ROS and the insurgence of inflammatory processes.[18−20] Interestingly, the healing effects of an aqueous ethanolic extract of *E. angustifolia* has been reported in 5-fluorouracil-induced oral mucositis in male golden hamsters.[21] Considering the possibility to consume the *E. umbellata* fruits, the antioxidant ability and the beneficial effects of their extracts and isolated compounds (**2** and **5**−**14**) in human gingival fibroblasts were evaluated for the first time. Furthermore, the ability of the most promising derivative, compound **6**, to decrease the transcription of lipopolysaccharide (LPS)-induced pro-inflammatory cytokines (IL-6 and IL-8) was also assessed.

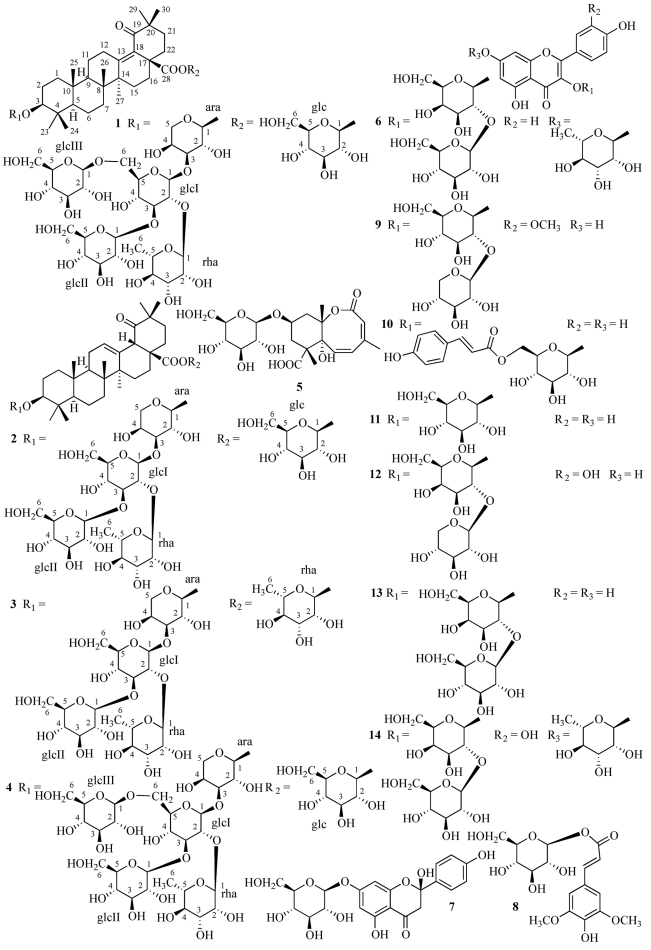

RESULTS AND DISCUSSION

The fruits of *E. umbellata* were defatted with *n*-hexane and then extracted with MeOH. The MeOH extract was partitioned between EtOAc, *n*-BuOH, and H_2O. The EtOAc and *n*-BuOH extracts, subjected to Isolera flash chromatography, Sephadex LH-20, and RP-HPLC separations, yielded in pure form five new (**1**−**5**) and nine known compounds (**6**−**14**). The chemical profiles of the EtOAc and *n*-BuOH extracts are shown in Figure 1.

The molecular formula of compound **1** was determined as $C_{65}H_{104}O_{32}$ by HRESIMS, showing a sodium adduct ion at *m*/*z* 1419.6357 $[M + Na]^+$. Analysis of the NMR data (Tables 1 and 2) confirmed the presence of 30 signals attributable to the aglycone moiety and 35 to the saccharide portion, establishing the presence of a bidesmosidic triterpenoid saponin. In the ESIMS data, fragments obtained in the negative and positive modes at *m*/*z* 1249 $[M - H - 146]^-$, 1071 $[M - H - 162 - 162]^-$, 1257 $[M + Na - 162]^+$, and 1095 $[M + Na - 162 - 162]^+$ suggested the presence of a triterpenoid saponin structure with at least one deoxyhexosyl and two hexosyl moieties. The ^1H NMR data of **1** displayed seven methyl singlets at δ_H 0.87, 0.94, 0.99, 1.06, 1.09, 1.10, and 1.27, a hydroxymethine at δ 3.18 (dd, J = 11.5, 4.3 Hz), and six anomeric protons at δ 4.33 (d, J = 7.4 Hz), 4.44 (d, J = 6.8 Hz), 4.68 (d, J = 7.7 Hz), 4.77 (1H, d, J = 7.5 Hz), 5.45 (d, J = 8.0 Hz), and 5.61 (d, J = 1.8 Hz). The ^{13}C NMR data suggested the structural features of 3-hydroxy-19-oxoolean-13-en-28 oic acid for the aglycone of compound **1** due to the presence of a hydroxymethine at δ_C 89.6 and an α,β-unsaturated carbonyl (δ_C 134.0, 153.3, and 211.0). This conclusion was supported by HMBC correlations between H_2-16−C-14, H_2-16−C-17, H_2-16−C-18, H_2-12−C-18, Me-29−C-19, Me-29−C-20, and Me-29−C-21.[21] The structure of the sugar moieties was deduced using 1D TOCSY, COSY, HSQC, and HMBC experiments, leading to recognition of four β-glucopyranosyl, an α-arabinopyranosyl, and an α-rhamnopyranosyl moiety. The chemical shifts of one glucose anomeric proton at δ_H 5.45 and δ_C 95.9 suggested this sugar moiety to be involved in an ester linkage with the C-28 carboxylic acid group at δ_C 174.2, and the HMBC correlation peak between $H\text{-}1_{glc}$−C-28 corroborated this substitution. Direct evidence of the sugar sequence at C-3 was derived from the HMBC correlations between $H\text{-}1_{ara}$−C-3, $H\text{-}1_{glcI}$−$C\text{-}3_{ara}$, $H\text{-}1_{rha}$−$C\text{-}2_{glcI}$, $H\text{-}1_{glcII}$−$C\text{-}3_{glcI}$, and $H\text{-}1_{glcIII}$−$C\text{-}6_{glcI}$. The assignment of the sugar configuration was obtained through hydrolysis of **1** with 1 N HCl followed by GC analysis through a chiral phase column of the monosaccharides treated with 1-(trimethylsilyl)-imidazole in pyridine. Thus, compound **1** was identified as 28-*O*-β-D-glucopyranosyl 3β-*O*-[β-D-glucopyranosyl-(1→6)]-[β-D-glucopyranosyl)-(1→3)]-[α-L-rhamnopyranosyl-(1→2)]-β-D-glucopyranosyl-(1→3)-α-L-arabinopyranosyl-19-oxoolean-13-en-28-oate.

Compound **2** showed a sodium adduct ion at *m*/*z* 1257.5826 $[M + Na]^+$, differing by 162 Da from **1**. In the ESIMS fragments obtained in the positive ion mode at *m*/*z* 1095 $[M + Na - 162]^+$, 1111 $[M + Na - 146]^+$, 933 $[M + Na - 162 - 162]^+$, 625 $[M + Na - 162 - 162 - 146 - 162]^+$, and 447 $[M + Na - 162 - 162 - 146 - 162 - 132 - 46]^+$ were consistent with the presence of a triterpenoid saponin with five sugar moieties comprising three hexosyl, one deoxyhexosyl, and one pentosyl unit. Analysis of the NMR data (Table 1) for the aglycone moiety showed the presence of

https://dx.doi.org/10.1021/acs.jnatprod.9b01030
J. Nat. Prod. 2020, 83, 626−637

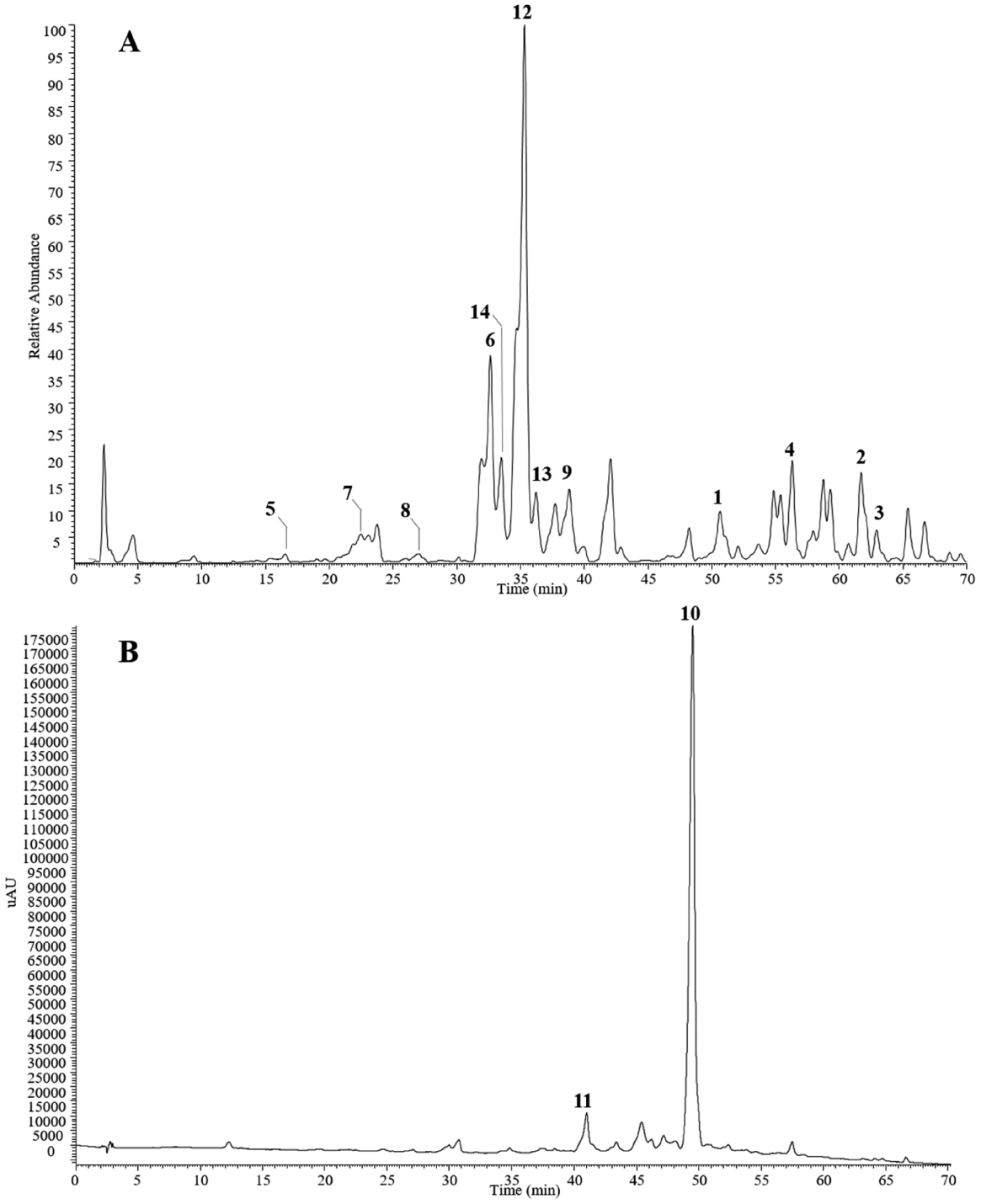

Figure 1. Chemical profiles of *Elaeagnus umbellata* fruit extracts. (A) HPLC-ESIMS of the *n*-BuOH extract registered in the negative ion mode. (B) HPLC/UV of the EtOAc extract registered at 350 nm. Peak numbers indicate the isolated compounds.

nine methylenes, seven methyls, four methines (one oxygenated), an sp^2 methine, seven quaternary carbons (one sp^2), a keto, and a hydroxy carbonyl carbon. The MS and NMR data displayed for the aglycone moiety eight indices of hydrogen deficiency. The ^{1}H NMR spectrum showed, in addition to signals corresponding to seven methyls, a hydroxymethine at δ 3.19 (dd, J = 12.0, 4.0 Hz) and an olefinic proton at δ 5.26 (t, J = 3.0 Hz). The HMBC spectrum showed correlations between Me-29 (δ 1.22) and C-19, C-20, and C-21 and between H-18 (δ 3.79) and C-12, C-16, C-18, C-19, and C-20. The spectroscopic features (Table 1) were in agreement with a 19-oxooleanolic acid as the aglycone of compound **2**. This triterpenoid aglycone structure is described here for the first time. Comparison of the spectroscopic data of the sugar portion of compounds **2** and **1** (Table 2) showed structural similarities: in particular, the saccharide chain of **2** differed from that of **1** only in the absence of the β-glucopyranosyl moiety linked at C-6 of glc I. The configuration of the saccharide units was assigned as reported for **1**. Thus, compound **2** was characterized as 28-*O*-β-D-glucopyranosyl 3β-*O*-β-D-glucopyranosyl-(1→3)-β-D-glucopyranosyl-(1→2)-

https://dx.doi.org/10.1021/acs.jnatprod.9b01030
J. Nat. Prod. 2020, 83, 626−637

Table 1. ^{1}H and ^{13}C NMR Data for Aglycones of Compounds 1, 2, and 5[a]

	1		2			5	
position	δ_H	δ_C	δ_H	δ_C	position	δ_H	δ_C
1a	1.77[b]	39.9	1.71[b]	39.0	2		174.0
1b	1.07, m		1.08[b]		3	5.91, s	126.6
2a	1.92[b]	27.0	2.05, m	26.5	4		140.0
2b	1.76[b]		1.74[b]		5	7.91, d (16.0)	133.8
3	3.18, dd (11.5, 4.3)	89.6	3.19, dd (12.0, 4.0)	89.5	6	6.25, d (16.0)	126.7
4		39.1		39.0	7		80.5
5	0.83, br d (11.7)	57.3	0.84, br d (11.5)	57.2	8		51.0
6a	1.64[b]	19.0	1.59[b]	19.0	9a	2.09, dd (14.0, 7.5)	39.1
6b					9b	1.93, dd (14.0, 11.0)	
7a	1.66[b]	34.3	1.68[b]	34.2	10	4.01, m	72.8
7b	1.41, m		1.41, m		11a	2.45, dd (14.4, 6.5)	39.0
8		43.0		40.0	11b	1.99, dd (14.4, 10.0)	
9	1.61[b]	52.2	1.71[b]	48.5	12		87.5
10		36.9		36.0	13	2.04, s	20.1
11a	1.61[b]	23.5	2.00[b]	24.1	14		178.0
11b			1.98[b]		15	1.12, s	14.0
12a	2.67, br dd (16.0, 12.0)	134.0	5.26, t (3.0)	129.4	16	1.40, s	18.2
12b	1.99, m				Glc-1	4.37, d (7.8)	103.0
13		153.3		133.0	2	3.16, br t (9.0)	74.6
14		45.0		41.8	3	3.26, t (9.5)	77.4
15a	1.92[b]	27.0	1.99[b]	28.0	4	3.30, t (9.5)	71.3
15b	1.76[b]		1.82, m		5	3.38, m	77.7
16a	2.15, ddd (14.3, 6.5, 3.8)	34.3	1.89[b]	27.0	6a	3.86, dd (12.0, 3.0)	62.2
16b	1.93[b]		1.62[b]		6b	3.68, dd (12.0, 5.0)	
17		53.1		50.0			
18		134.0	3.79, s	56.8			
19		211.0		216.5			
20		45.5		44.0			
21a	1.85, ddd (17.0, 14.3, 3.8)	36.6	1.93[b]	35.2			
21b	1.65[b]		1.77[b]				
22a	2.30, ddd (14.3, 6.6, 3.3)	32.0	2.26, ddd (15.0, 11.0, 4.0)	31.0			
22b	1.63[b]		1.80[b]				
23	1.06, s	28.0	1.07, s	28.1			
24	0.87, s	17.0	0.89, s	17.0			
25	0.99, s	17.0	1.00, s	16.0			
26	0.94, s	14.0	0.85, s	17.5			
27	1.27, s	21.0	0.97, s	23.0			
28		174.2		175.0			
29	1.09, s	26.5	1.22, s	27.0			
30	1.10, s	25.5	1.11, s	25.6			

[a]Spectra were recorded in methanol-d_4 at 600 MHz (^{1}H) and 150 MHz (^{13}C). J values are in parentheses and reported in Hz; chemical shifts are given in ppm; assignments were confirmed by 1D-TOCSY, COSY, HSQC, and HMBC experiments. [b]Overlapped signal.

[α-L-rhamnopyranosyl]-(1→3)-α-L-arabinopyranosyl-19-oxooleanolate.

Compound **3** ($C_{59}H_{94}O_{26}$), isolated in a small amount, exhibited a sodium adduct ion at m/z 1241.5990 $[M + Na]^+$, as well as a fragment peak at m/z 1095.6798 $[M + Na - 146]^+$ corresponding to the loss of a deoxyhexosyl unit. Analysis of its NMR spectroscopic data (Table 2) and comparison with those of saponin **2** showed that the aglycone moiety and the sugar chain at C-3 of **3** were the same as those of **2**, while the sugar moiety at C-28 was different. The presence of an anomeric proton at δ_H 6.00 and at δ_C 95.5 belonging to a terminal rhamnopyranosyl moiety suggested this sugar to be linked at C-28. This assumption was substantiated by the HMBC correlation between H-1_{rha} (δ_H 6.00) and C-28 (δ_C 175.0). The configuration of the saccharide units was determined as reported for **1**. The structure of **3** was thus established as 28-*O*-α-L-rhamnopyranosyl 3β-*O*-D-glucopyranosyl-(1→3)-β-D-glucopyranosyl-(1→2)-[α-L-rhamnopyranosyl]-(1→3)-α-L-arabinopyranosyl-19-oxooleanolate.

Compound **4** was isolated in a trace amount. Its HRESIMS data in the positive ion mode showed an $[M + Na]^+$ ion at m/z 1419.6390, corresponding to a molecular formula of $C_{65}H_{104}O_{32}$, and hence was shown to be an isomer of **1**. The HRESIMS/MS data revealed the presence of fragments at m/z 1257.7781 $[M + Na - 162]^+$ and 1095.6188 $[M + Na - 162 - 162]^+$ due to the subsequent loss of two hexosyl moieties. Comparison of its NMR spectroscopic data with those of saponins **1**−**3** showed **4** to have the same aglycone as **2**, while its saccharidic chains at C-3 and C-28 were identical to those of **1**. The aglycone moiety of compound **1** could be an artifact of **4**. The double-bond rearrangement could be due to the formation of a conjugated α,β-unsaturated carbonyl system.

https://dx.doi.org/10.1021/acs.jnatprod.9b01030
J. Nat. Prod. 2020, 83, 626−637

Table 2. ^{1}H and ^{13}C NMR Data for Sugar Moieties of Compounds 1−3[a]

	1		2		3	
position	δ_H	δ_C	δ_H	δ_C	δ_H	δ_C
ara-1 at C-3	4.44, d (6.8)	105.7	4.44, d (6.7)	105.8	4.44, d (6.8)	106.0
2	3.91, dd (9.0, 6.8)	75.0	3.93, dd (9.0, 6.7)	75.0	3.93, dd (9.0, 6.8)	75.1
3	3.95, dd (9.0, 2.0)	83.0	3.91, dd (9.0, 3.0)	82.7	3.91, dd (9.0, 2.5)	82.3
4	4.08, m	70.0	4.08, m	70.0	4.07, m	71.0
5a	3.88, dd (12.0, 2.0)	66.2	3.87, dd (12.0, 2.5)	66.0	3.90, dd (12.0, 2.0)	66.5
5b	3.65, dd (12.0, 4.0)		3.61, dd (12.0, 4.0)		3.62, dd (12.0, 4.5)	
glc I-1	4.68, d (7.7)	103.0	4.66, d (7.5)	102.8	4.68, d (8.0)	102.9
2	3.66[b]	77.0	3.64[b]	77.8	3.60, dd (9.5, 8.0)	77.8
3	3.65[b]	83.4	3.65[b]	83.3	3.66, t (9.5)	83.6
4	3.28, t (9.5)	71.0	3.40, t (9.5)	70.6	3.39, t (9.5)	71.0
5	3.55, m	76.7	3.33, m	77.9	3.31, m	78.0
6a	4.20, dd (12.0, 3.0)	70.0	3.88, dd (12.0, 3.5)	62.0	3.88, dd (12.0, 3.0)	62.4
6b	3.72, dd (12.0, 5.0)		3.72, dd (12.0, 5.0)		3.72, dd (12.0, 4.5)	
rha-1	5.61, d (1.8)	101.0	5.62, d (1.5)	100.7	5.64, d (1.8)	100.0
2	3.95, dd (3.0, 1.8)	72.0	3.96, dd (3.0, 1.5)	72.0	3.96, dd (3.0, 1.8)	72.1
3	3.73, dd (9.0, 3.0)	72.0	3.74, dd (9.0, 3.0)	71.8	3.72, dd (9.0, 3.0)	72.0
4	3.45, t (9.0)	74.0	3.45, t (9.0)	73.5	3.47, t (9.0)	73.0
5	4.07, m	70.0	4.10, m	70.0	4.09, m	70.5
6	1.26, d (6.5)	17.0	1.25, d (6.8)	17.4	1.28, d (6.5)	18.0
glc II-1	4.77, d (7.5)	105.7	4.78, d (7.5)	105.3	4.79, d (7.5)	105.6
2	3.38, dd (9.5, 7.5)	75.0	3.40[b]	75.0	3.39, dd (9.0, 7.5)	75.6
3	3.34, t (9.5)	78.0	3.42, t (9.0)	78.0	3.44, t (9.0)	78.0
4	3.40, t (9.5)	70.0	3.40[b]	71.0	3.43, t (9.0)	71.0
5	3.36, m	77.0	3.33, m	77.9	3.31, m	78.3
6a	3.93, dd (12.0, 3.0)	62.0	3.90, dd (12.0, 2.5)	62.1	3.93, dd (12.0, 3.0)	62.1
6b	3.75, dd (12.0, 4.5)		3.80, dd (12.0, 4.5)		3.77, dd (12.0, 5.0)	
glc III-1	4.33, d (7.4)	104.9				
2	3.23, dd (9.0, 7.4)	75.0				
3	3.35, t (9.0)	77.0				
4	3.28, t (9.0)	71.0				
5	3.41, m	77.0				
6a	3.90, dd (12.0, 3.0)	62.0				
6b	3.69, dd (12.0, 5.0)					
glc-1 at C-28	5.45, d (8.0)	95.9	5.46, d (8.0)	95.7		
2	3.29, dd (9.5, 8.0)	75.0	3.35, dd (9.5, 8.0)	73.4		
3	3.41[b]	77.7	3.33, t (9.5)	77.9		
4	3.40[b]	70.0	3.40[b]	70.6		
5	3.36, m	77.0	3.40[b]	78.0		
6a	3.83, dd (12.0, 3.0)	62.0	3.86, dd (12.0, 2.5)	62.0		
6b	3.70, dd (12.0, 4.5)		3.72, dd (12.0, 5.0)			
rha-1 at C-28					6.00, d (1.8)	95.5
2					3.96, dd (3.0, 1.8)	72.1
3					3.72, dd (9.5, 3.0)	72.0
4					3.44, t (9.5)	73.0
5					4.09, m	70.5
6					1.24, d (6.0)	18.0

[a]Spectra were recorded in methanol-d_4 at 600 MHz (^{1}H) and 150 MHz (^{13}C). J values are in parentheses and reported in Hz; chemical shifts are given in ppm; assignments were confirmed by COSY, 1D-TOCSY, HSQC, and HMBC experiments. [b]Overlapped signal.

Therefore, the structure 28-*O*-*β*-D-glucopyranosyl 3-*O*-[*β*-D-glucopyranosyl-(1→6)]-[*β*-D-glucopyranosyl)-(1→3)]-[*α*-L-rhamnopyranosyl-(1→2)]-*β*-D-glucopyranosyl-(1→3)-*α*-L-arabinopyranosyl-19-oxooleanolate was assigned to compound **4**.

Compound **5** had the molecular formula $C_{21}H_{30}O_{11}$ as determined by HRESIMS (m/z 481.1666 $[M + Na]^+$). Its ESIMS data recorded in the negative ion mode displayed fragments at m/z 413 $[M - H - 44]^-$, 295 $[M - H - 162]^-$, 251 $[M - H - 162 - 44]^-$, 233 $[M - H - 162 - 18 - 44]^-$, and 189 $[M - H - 162 - 18 - 44 - 44]^-$, due to the subsequent loss of CO_2, a hexosyl unit, H_2O, and a second CO_2 molecule. These data supported the presence of two carboxylic groups in the structure of **5**. The ^{13}C NMR data of **5** (Table 1) showed 21 signals, of which 15 were assigned to a sesquiterpenoid moiety and six to the sugar portion. The signals of the aglycone moiety were sorted into three methyls, two methylenes, three sp^2 methines, a hydroxymethine, two quaternary carbons, two oxygenate tertiary carbons, a hydroxycarbonyl carbon, and an ester carbonyl. The ^{1}H NMR data (Table 1) displayed three methyl singlets at δ 1.12,

https://dx.doi.org/10.1021/acs.jnatprod.9b01030
J. Nat. Prod. 2020, 83, 626−637

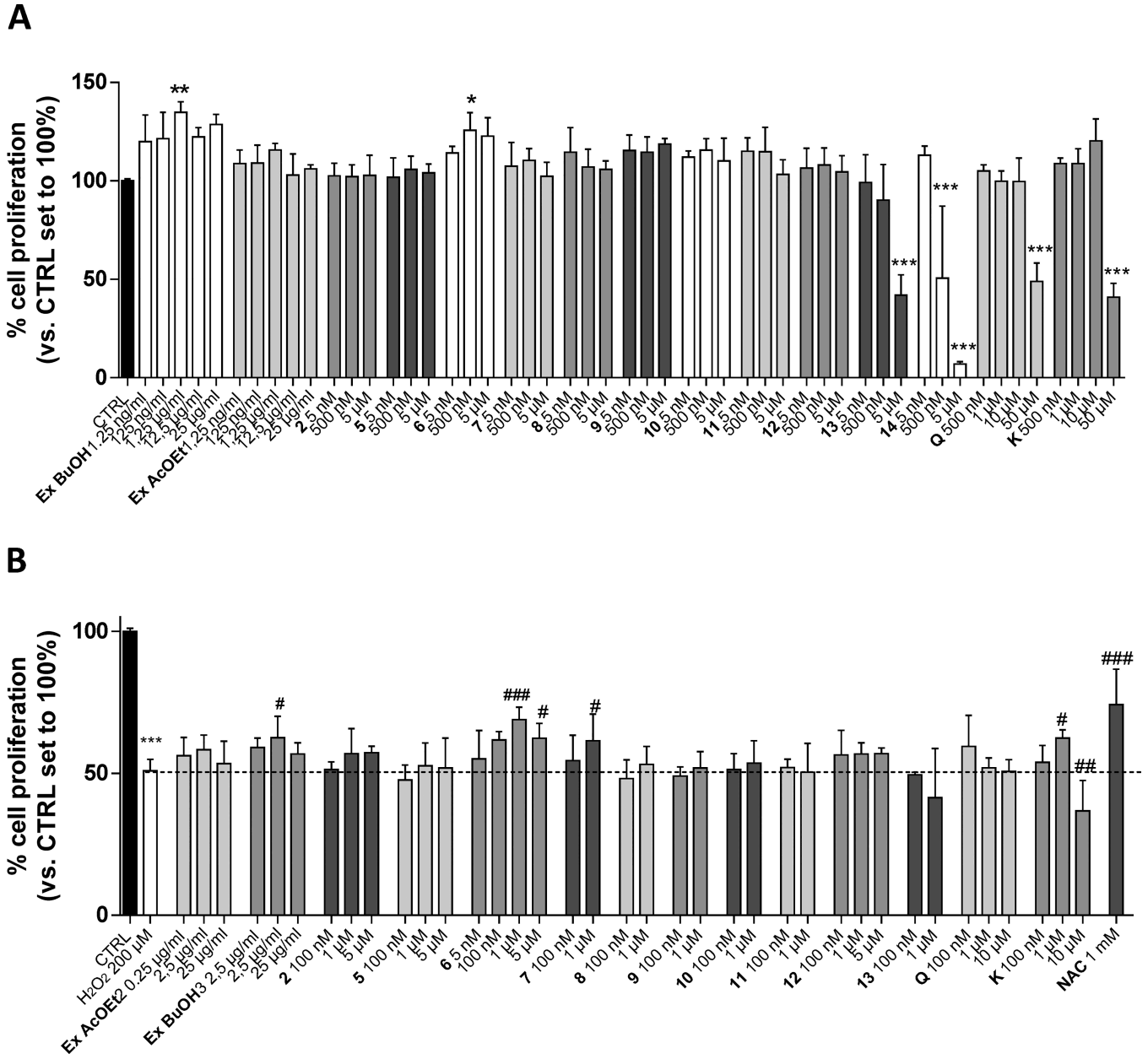

Figure 2. Protective effects of *Elaeagnus umbellata* extracts and isolated compounds on hGF. Human GF cells were treated with different concentrations of Ex EtOAc, Ex BuOH, compounds **2**, **5**, and **6**−**14**, quercetin (**Q**), kaempferol (**K**), or NAC (1 mM) in the absence (A) or presence (B) of H_2O_2 (200 μM) for 72 h in complete medium. In the end, the MTS assay was performed. Data are expressed as percentage of cell proliferation compared to the control, which was set to 100%. Each bar represents the mean ± SD of three replicates from two independent experiments. The significance of the differences was determined by one-way ANOVA, which was followed by Bonferroni's post-test: *$p < 0.05$, **$p < 0.01$, ***$p < 0.001$, vs CTRL; $^{\#}p < 0.05$, $^{\#\#}p < 0.01$, $^{\#\#\#}p < 0.001$, vs H_2O_2.

1.40, and 2.04, the latter having a chemical shift typical of an allylic methyl, together with signals of three olefinic protons at δ_H 5.91 (s), 6.25 (d, J = 16.0 Hz), and 7.91 (d, J = 16.0 Hz), a hydroxymethine (δ 4.01, m), and an anomeric proton (δ 4.37, d, J = 7.8 Hz). The COSY experiment indicated two spin systems for the aglycone corresponding to the sequence $-CH_2-CHOH-CH_2-$ and $-CH{=}CH-C-CH-$, respectively. The HSQC experiment allowed the assignments of all protons linked to the respective carbons, to identify the β-glucopyranosyl moiety, while the HMBC spectrum was crucial to identify the aglycone as amygdalactone.[22] The HMBC correlation between H-1_{glc} at δ_H 4.37 and C-10 at δ_C 72.8 confirmed the glucosyl substitution site. On the basis of these data, compound **5** was identified as 10-*O*-β-D-glucopyranosylamygdalactone (**5**). The aglycone amygdalactone was isolated before only from *Prunus amygdalus*[22] and *Cinnamomum cassia*.[23]

Compounds **6**−**14** were also purified and characterized as kaempferol 3-*O*-β-D-glucopyranosyl-(1→2)-β-D-galactopyranoside-7-*O*-α-L-rhamnopyranoside (**6**),[24] 2-hydroxynaringenin 7-*O*-β-D-glucopyranoside (**7**),[25] 1-*O*-(*trans*-sinapoyl)-β-D-glucopyranoside (**8**),[26] isorhamnetin 3-*O*-α-L-xylopyranosyl-(1→2)-β-D-glucopyranoside (**9**),[27] tiliroside (**10**),[28] kaempferol 3-*O*-β-D-glucopyranoside (**11**),[29] quercetin 3-*O*-α-L-xylopyranosyl-(1→2)-β-D-galactopyranoside (**12**),[30] kaempferol 3-*O*-β-D-glucopyranosyl-(1→2)-β-D-galactopyranoside (**13**),[31] and

https://dx.doi.org/10.1021/acs.jnatprod.9b01030
J. Nat. Prod. 2020, 83, 626−637

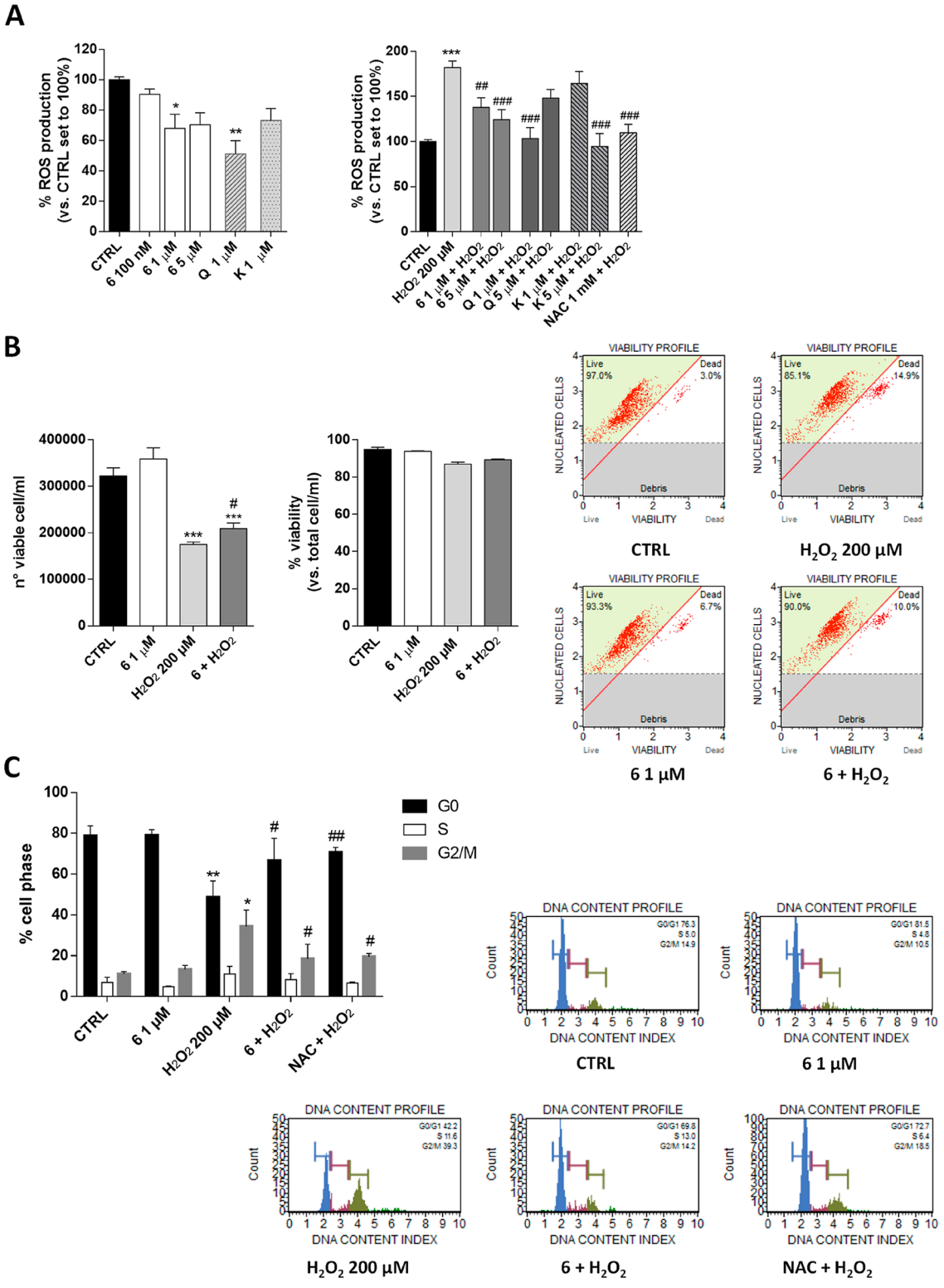

Figure 3. Effect of compound **6** on ROS production, cell death, and cell cycle progression. hGF cells were treated with different concentrations of compound **6**, quercetin (**Q**), kaempferol (**K**), or NAC as indicated, alone or in the presence of H_2O_2 (200 μM) for 72 h in complete medium. The ROS levels were evaluated by H_2DCFDA (A). Data are expressed as the percentage of ROS with respect to the amount in the CTRL set to 100%. Each bar represents the mean ± SD of three replicates from two independent experiments. (B) Flow cytometry analysis of cell death was performed as described in the Experimental Section. Data are reported as the number of cells/mL and as percentage of cell death. Each bar represents the mean ± SD of two replicates from two independent experiments. Representative histograms are shown. (C) Flow cytometry analysis of the cell cycle was performed as described in the Experimental Section. Data are reported as the percentage of cells in each cell phase. Each bar represents the mean ± SD of two replicates from two independent experiments. Representative histograms are shown. The significance of the differences was determined by one-way ANOVA, which was followed by Bonferroni's post-test: $^{*}p < 0.05$, $^{**}p < 0.01$, $^{***}p < 0.001$, vs CTRL; $^{\#}p < 0.05$, $^{\#\#}p < 0.01$, $^{\#\#\#}p < 0.001$ vs H_2O_2.

https://dx.doi.org/10.1021/acs.jnatprod.9b01030
J. Nat. Prod. 2020, 83, 626−637

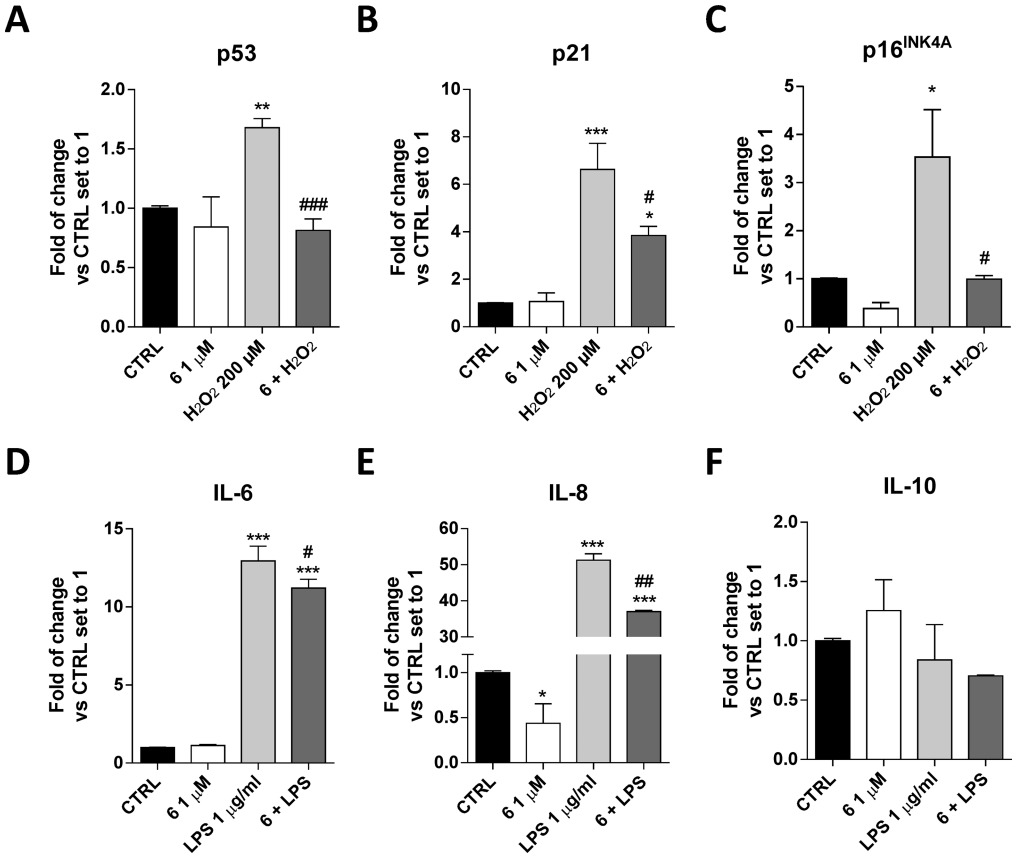

Figure 4. Compound **6** modulation of senescence-associated and cytokine gene expression in hGF. hGF cells were treated with different concentrations of compound **6** alone or in the presence of H_2O_2 (200 μM) or LPS (1 μg/mL) for 72 h in complete medium. Then, the mRNA levels of p53 (A), p21 (B), $p16^{INK4A}$ (C), IL-6 (D), IL-8 (E), and IL-10 (F) were quantified using real-time RT-PCR analysis. Data are expressed as the fold change versus the CTRL, which was set to 1, and are presented as the mean values ± SD of two independent experiments performed in duplicate. The significance of the differences was determined by one-way ANOVA, which was followed by Bonferroni's post-test: $^{*}p < 0.05$, $^{**}p < 0.01$, $^{***}p < 0.001$ vs CTRL; $^{\#}p < 0.05$, $^{\#\#}p < 0.01$, $^{\#\#\#}p < 0.001$ vs H_2O_2 or LPS.

quercetin 3-*O*-β-D-glucopyranosyl-(1→2)-β-D-galactopyranoside-7-*O*-α-L-rhamnopyranoside (**14**),[27] by comparison of their NMR and MS data to literature data.

Compound **2**, as a representative saponin, compounds **5**−**14**, and the EtOAc (Ex EtOAc) and *n*-BuOH (Ex BuOH) extracts were screened for their potential proliferative effects on human gingival fibroblast (hGF) using the MTS assay (Figure 2A). Among the compounds, **13** and **14** produced a significant decrease in cell proliferation when used at micromolar concentrations. Conversely, Ex BuOH and compound **6** (1 μM) were able to significantly increase the hGF proliferation to 122.3 ± 4.8% and 125.6 ± 9.1%, respectively, showing a beneficial effect of compound **6** on hGF. Challenging the fibroblast with low concentrations of quercetin (**Q**) and kaempferol (**K**) did not affect the proliferation of hGF. These data are in accordance with the ability of kaempferol glycosides to increase keratinocyte proliferation more than kaempferol itself.[32] Conversely, a high concentration (50 μM) of **Q** and **K** caused a significant decrease in cell proliferation. The treatment with a high concentration of H_2O_2 (millimolar range) causes cell death in different cellular models. However, the use of a micromolar concentration of H_2O_2 for a prolonged period induces DNA damage, cell cycle arrest, and the expression of senescence-associate protein (p53, p21, and p16).[33] Herein, we used a low concentration of H_2O_2 (200 μM) that better reproduces the effects of ROS in periodontitis and mucositis. The ability of all the tested compounds to counteract the decrease of proliferation induced by H_2O_2 was evaluated using the MTS assay (Figure 2B). Challenging hGF cells with H_2O_2 for 72 h significantly decreased the proliferation (50.9 ± 4.0%, $p < 0.001$ vs CTRL), and these effects were counteracted by *N*-acetylcysteine (NAC) tested as reference antioxidant molecule (74.1 ± 12.6%, $p < 0.001$ vs CTRL).[34] Interestingly, Ex BuOH counteracted the decrease of cell proliferation (62.5 ± 7.5%, $p < 0.05$ vs CTRL), and compound **6** produced a more robust effect (68.8 ± 4.4%, $p < 0.01$ vs CTRL).

Successively, we extensively investigated the effects of compound **6** on hGF as a new potential biological activity of a rare flavonoid glycoside. The correct balance of intracellular ROS level positively regulates physiological functions, including signal transduction, gene expression, and proliferation, favoring adaptive responses and longevity. In contrast, the uncontrolled production of ROS induces ineffective adaptive responses, contributing to aging phenomena.[35] In this respect, the antioxidant ability of compound **6** was investigated in the absence or presence of H_2O_2 using H_2DCFDA, which is the reduced form of fluorescein used as an indicator of intracellular ROS levels (Figure 3A). Compound **6** alone decreased the intracellular ROS concentration ($p < 0.05$). Despite the fact that this effect was similar to that obtained with **K**, a low concentration of **Q** produced a more robust effect, in accordance with its antioxidant effects reported in other cell lines.[36] Interestingly, compound **6**

https://dx.doi.org/10.1021/acs.jnatprod.9b01030
J. Nat. Prod. 2020, 83, 626−637

significantly counteracted the ROS production induced by H_2O_2 (181.9 ± 7.4% H_2O_2, 124.2 ± 11.3% **6**, $p < 0.001$).[37,38] This effect was similar to that obtained for NAC (109.7 ± 9.4%, $p < 0.001$ vs H_2O_2). Overall, these results indicated that the flavonol derivate of *E. umbellata* slightly alters the balance of intracellular ROS in physiological conditions, but could effectively counteract the stress effects produced by the external stimuli.

The modification of cell proliferation could be due to the induction of cell death or a blockade of the cell cycle. In order to extensively investigate the well-being activity of compound **6**, a live/death cell count assay was performed (Figure 3B). The results demonstrated that treatment with H_2O_2 did not induce significant cell death, in accordance with the use of a low concentration. Similarly, the treatment with compound **6** alone or in combination with H_2O_2 did not alter the number of dead cells. Compound **6** alone did not produce a significant increase in cell number (322 400 ± 39431, CTRL; 358 800 ± 53942); however, it significantly counteracted the decrease of cell number induced by H_2O_2 (175 200 ± 11 777, H_2O_2; 209 500 ± 23502, **6** + H_2O_2; $p < 0.05$), in accordance with the results obtained for cell proliferation (Figure 2). Next, a flow cytometry analysis was performed to investigate the cell cycle progression (Figure 3C). hGF cells in the absence of H_2O_2 treatment showed a typical cell cycle distribution with most cells in G0/G1 phase (78.7 ± 4.9%). The treatment with H_2O_2 significantly increased the number of cells in the S and G2/M phases (from 11.1 ± 1.2% to 34.3 ± 8.1%; $p < 0.05$), as well as decreased the number of cells in the G0/G1 phase (48.6 ± 7.9%; $p < 0.001$), in accordance with the reported ability of ROS to produce a G2/M cell cycle blockade.[39] This modification was almost completely counteracted by NAC (70.6 ± 2.5%, G0/G1; $p < 0.01$; 19.5 ± 1.2%, G2/M; $p < 0.05$). Interestingly, compound **6** counteracted the cell cycle blockade, increased the cells in the G0/G1 phase (66.6 ± 10.9%; $p < 0.05$), and reduced those in the G2/M phase (18.5 ± 7.1%; $p < 0.05$).

So far, oxidative stress has been associated with senescence and growth arrest, and it has been shown that these phenomena depend functionally on the expression of different proteins such as $p16^{INK4}$, the cyclin-dependent kinase (CDK) inhibitor p21, and tumor suppressor p53.[40] In this respect, the gene expression of these proteins was evaluated by means of real-time reverse transcription (RT)-PCR (Figure 4A−C). Compound **6** "per se" did not alter the p21 and p53 transcription and produced only a slight decrease of p16 in accordance with its ability to promote the hGF cell proliferation. The oxidative stress caused a significant increase of p53, p21, and p16 gene expression, in accordance with the H_2O_2-induced cell blockage. Compound **6** counteracted the effects of H_2O_2, decreasing the transcription of all the proteins.

Periodontitis and mucositis are also characterized by the presence of high levels of pro-inflammatory cytokines that are released in response to extracellular stimuli (e.g., bacteria) by different types of cells such as fibroblasts.[41] Thus, to further characterize the beneficial activity of compound **6** on gingival cells, the gene expression of pro-inflammatory (interleukin-6, IL6, and interleukin-8, IL-8) and anti-inflammatory (interleukin-10, IL-10) cytokines was evaluated using a real-time RT-PCR analysis (Figure 4D−F). Challenging cells with LPS (1 μg/mL) promoted the transcription of IL-6 and IL-8 and the decrease of IL-10. Compound **6** restored the balance of the released cytokines in favor of a lower inflammatory status; in fact, it reduced the expression of IL-6 and IL-8 and increased the expression of IL-10.

Compound **6** has recently been reported as a dipeptidyl peptidase IV (DPP-IV) inhibitor,[42] and different kaempferol glycosides have been reported to increase keratinocyte proliferation[32] and protect red blood cells and neutrophils from DNA damage;[36,43] however, its effect on gingival tissue has not yet been reported.

Compound **6** counteracted the negative effects of oxidative stress and decreased the gene expression of pro-inflammatory cytokines. Poor absorption of some flavonoids and flavonoid glycosides is a major limitation for use of flavonoids as systemic nutraceuticals.[44] However, the ability of a flavonoid to act from the extracellular compartment modifying the membrane composition and interacting with different membrane receptors has recently been reported.[45] The exact mechanism of action of compound **6** is still unclear; however we could speculate that the glycoside or its metabolites could interact with extracellular cell components, modifying the hGF oxidative state and decreasing the inflammatory status. In conclusion, these results highlight a new property of a flavonoid glycoside as a possible local protective agent against oxidative stress and inflammatory stimuli in gingival tissue.

EXPERIMENTAL SECTION

General Experimental Procedures. Optical rotations were measured by an Atago AP-300 digital polarimeter with a 1 dm microcell and a sodium lamp (589 nm). NMR experiments were recorded on a Bruker DRX-600 spectrometer at 300 K (Bruker BioSpin, Germany), acquiring the spectra in methanol-d_4.[46] HRESIMS data were obtained in the positive and negative ion mode on an LTQ Orbitrap XL mass spectrometer (Thermo Fisher Scientific) and Q-TOF Premier spectrometer equipped with a nanospray ion source (Waters, USA). ESIMS data were acquired on an LCQ Advantage ThermoFinnigan spectrometer (ThermoFinnigan, USA), equipped with Xcalibur software. LC-PDA/UVvis/ESIMS/MS analyses were performed on a Synergi Fusion-RP column (4.6 × 150 mm, 4 μm, flow rate 0.8 mL/min, Phenomenex, Italy), eluting with a mixture of MeOH (solvent A) and formic acid in water 0.1% v/v (solvent B) and using a linear gradient of increasing 5% to 75% MeOH within 70 min. MS parameters were optimized as previously reported.[47] Columns chromatography was performed over Sephadex LH-20 and an Isolera Biotage flash purification system (flash silica gel 60 SNAP cartridge). HPLC separations were carried out using a Shimadzu LC-8A series pumping system equipped with a Shimadzu RID-10A refractive index detector and Shimadzu injector (Shimadzu Corporation, Japan) on a C_{18} μ-Bondapak column (30 cm × 7.8 mm, 10 mm, flow rate 2.0 mL/min). TLC separations were conducted using silica gel 60 F_{254} (0.20 mm thickness) plates (Merck, Germany) and $Ce(SO_4)_2$−H_2SO_4 as spray reagent (Sigma-Aldrich, Italy). GC analysis was performed using a Dani GC 1000 instrument on a L-CP-Chirasil-Val column (0.32 mm × 25 m), working with the following temperature program: 100 °C for 1 min, ramp of 5 °C/min up to 180 °C; injector and detector temperature 200 °C; carrier gas N_2 (2 mL/min); detector dual FID; split ratio 1:30; injection 5 μL.

Plant Material. The ripe fruits of *Elaeagnus umbellata* Thunb. were collected in October 2016 in Livorno (Italy) and identified by Prof. Fabiano Camangi. A voucher specimen (N.A. 5472 *Elaeagnus umbellata*/026677) was deposited at Herbarium Horti Botanici Pisani (Pisa, Italy).

Extraction and Isolation. Dried and powdered whole berries of *E. umbellata* (400.0 g) were defatted with *n*-hexane and extracted for 48 h with MeOH by exhaustive maceration (3 × 2.5 L), to give 137.7 g of extract. Dried MeOH extract was dissolved in water and partitioned with EtOAc and *n*-BuOH, successively, to yield 5.0 and 1.8 g of the respective residues. The *n*-BuOH extract was subjected to Sephadex LH-20 column chromatography (3 × 70 cm) using MeOH

https://dx.doi.org/10.1021/acs.jnatprod.9b01030
J. Nat. Prod. 2020, 83, 626−637

as eluent (flow rate 0.8 mL/min), collecting fractions of 8 mL that were grouped by thin-layer chromatography (TLC) into 10 major fractions (A_1–J_1). Fractions A_1 (25.5 mg), B_1 (35.5 mg), and C_1 (65.0 mg) were separately subjected to RP-HPLC with MeOH–H_2O (3:2) to yield compounds **4** (0.8 mg, t_R 16 min) and **1** (1.8 mg, t_R 41 min) from fraction A_1, compounds **2** (0.7 mg, t_R 35 min) and **1** (1.2 mg, t_R 41 min) from fraction B_1, and compounds **2** (1.8 mg, t_R 35 min) and **3** (1.1 mg, t_R 55 min) from fraction C_1. Fractions E_1 (115.0 mg) and G_1 (104.0 mg) were individually chromatographed by RP-HPLC with MeOH–H_2O (3.5:6.5) to give compound **5** (1.9 mg, t_R 8 min) from fraction E_1 and compounds **8** (1.0 mg, t_R 12 min), **7** (3.2 mg, t_R 16 min), **14** (4.5 mg, t_R 31 min), and **13** (3.7 mg, t_R 57 min) from fraction G_1. Fractions F_1 (63.2 mg) and I_1 (25.0 mg) were separately purified by RP-HPLC with MeOH–H_2O (2:3) to afford compound **6** (3.8 mg, t_R 16 min) from fraction F_1 and compound **9** (1.8 mg, t_R 44 min) from fraction I_1. Fraction J_1 (67.1 mg) contained pure compound **12**.

The EtOAc fraction was subjected to flash silica gel CC using an Isolera Biotage (SNAP 340 g column, flow rate 90 mL/min), eluting with $CHCl_3$, followed by increasing concentrations of MeOH in $CHCl_3$ (between 1% and 100%), collecting fractions of 27 mL, which were grouped by TLC into four major fractions (A_2–D_2). Fractions B_2 (69.0 mg) and C_2 (105.6 mg) were subjected to RP-HPLC with MeOH–H_2O (5.5:4.5) to yield compound **10** (1.7 mg, t_R 31 min) from fraction B_2 and compounds **11** (2.8 mg, t_R 17 min) and **10** (11.4 mg, t_R 37 min) from fraction C_2.

*Compound (**1**):* amorphous powder; $[\alpha]_D^{25}$ −8 (*c* 0.1, MeOH); ^{1}H and ^{13}C NMR data of the aglycone moiety, see Table 1; ^{1}H and ^{13}C NMR of the sugar moieties, see Table 2; ESIMS *m*/*z* 1395 $[M - H]^-$, 1249 $[M - H - 146]^-$, 1071 $[M - H - 162 - 162]^-$, 1419 $[M + Na]^+$, 1257 $[M + Na - 162]^+$, 1095 $[M + Na - 162 - 162]^+$; HRESIMS *m*/*z* 1419.6357 $[M + Na]^+$, 1257.5852 $[M + Na - 162]^+$ (calcd for $C_{65}H_{104}O_{32}Na$ 1419.6403).

*Compound (**2**):* amorphous powder; $[\alpha]_D^{25}$ −10.1 (*c* 0.1, MeOH); ^{1}H and ^{13}C NMR data of the aglycone moiety, see Table 1; ^{1}H and ^{13}C NMR of the sugar moieties, see Table 2; ESIMS *m*/*z* 1257 $[M + Na]^+$, 1095 $[M + Na - 162]^+$, 1111 $[M + Na - 146]^+$, 933 $[M + Na - 162 - 162]^+$, 625 $[M + Na - 162 - 162 - 146 - 162]^+$, 447 $[M + Na - 162 - 162 - 146 - 162 - 132 - 46]^+$; HRESIMS *m*/*z* 1257.5826 $[M + Na]^+$, 1095.6554 $[M + Na - 162]^+$ (calcd for $C_{59}H_{94}O_{27}Na$ 1257.5875).

*Compound (**3**):* amorphous powder; $[\alpha]_D^{25}$ −21 (*c* 0.1, MeOH); ^{1}H and ^{13}C NMR data of the aglycone moiety were superimposable to those reported for **2**; ^{1}H and ^{13}C NMR of the sugar moieties, see Table 2; HRESIMS *m*/*z* 1241.5990 $[M + Na]^+$, 1095.6798 $[M + Na - 146]^+$ (calcd for $C_{59}H_{94}O_{26}Na$ 1241.5926).

*Compound (**4**):* amorphous powder; $[\alpha]_D^{25}$ −7 (*c* 0.1, MeOH); ^{1}H and ^{13}C NMR data of the aglycone moiety were superimposable to those reported for **2**; ^{1}H and ^{13}C NMR of the sugar moieties were superimposable to those reported for **1**; HRESIMS *m*/*z* 1419.6390 $[M + Na]^+$, 1257.7781 $[M + Na - 162]^+$, 1095.6188 $[M + Na - 162 - 162]^+$ (calcd for $C_{65}H_{104}O_{32}Na$ 1419.6403).

*Compound (**5**):* amorphous powder; $[\alpha]_D^{25}$ −25 (*c* 0.1, MeOH); ^{1}H and ^{13}C NMR, see Tables 1 and 2; ESIMS *m*/*z* 457 $[M - H]^-$, 413 $[M - H - 44]^-$, 295 $[M - H - 162]^-$, 277 $[M - H - 180]^-$, 251 $[M - H - 162 - 44]^-$, 233 $[M - H - 162 - 18 - 44]^-$, 189 $[M - H - 162 - 18 - 44 - 44]^-$, 481 $[M + Na]^+$, 463 $[M + Na - 18]^+$, 437 $[M + Na - 44]^+$; HRESIMS *m*/*z* 481.1666 $[M + Na]^+$ (calcd for $C_{21}H_{30}O_{11}Na$ 481.1680).

Acid Hydrolysis of Compounds 1–5. Acid hydrolysis of compounds **1**–**5** was performed as reported previously.[39] D-Glucose, L-rhamnose, and L-arabinose were identified as the sugar unit in each case by comparison with the retention times of authentic samples.

Cell Culture. Human gingival fibroblast cells were purchased from CLS Cell Line Service GmbH (Germany), lot. number 300703-1541SF. Cells were maintained in DMEM-F12 supplemented with HEPES, 5% FBS, 2 mM L-glutamine, 100 U/mL penicillin, and 100 mg/mL streptomycin at 37 °C in 5% CO_2. Cells were used between passage 4 and 7.

Cell Proliferation Assay. hGF cells were seeded in 96-well microplates (1500 cells/well) in complete medium. After 24 h the medium was changed to noncomplete medium and cells were starved for 6 h. Then, cells were treated with test extracts and compounds at different concentrations (5 nM to 50 μM) in the absence or in the presence of H_2O_2 (200 μM) for 72 h. Extracts and compounds were solubilized in DMSO, and the final concentration of DMSO was 0.5%. Cell proliferation was evaluated using the MTS assay (CellTiter 96 AQueous One Solution cell proliferation assay kit; Promega) according to the manufacturer's instruction. The absorbance at 490 nm was measured with an automated plate reader (EnSight, PerkinElmer).

ROS Production. The intracellular ROS level was determined using the fluorogenic probe $DCFH_2$-DA (Molecular Probes, Invitrogen) as was previously reported.[48] Briefly, hGF cells were seeded in a 96-well microplate (5000 cells/well) and treated with compound **6**, **Q**, or **K** (1–5 μM) in the absence or in the presence of H_2O_2 (200 μM) for 72 h. Then, cells were incubated in phosphate-buffered saline (PBS)–glucose containing 50 μM $DCFH_2$-DA for 30 min. The medium was removed and replaced with PBS/glucose. The fluorescence intensity of DCF was measured with an automated plate reader (EnSight, PerkinElmer), with wavelengths of 485 nm (excitation) and 520 nm (emission). The cells were fixed with 3% paraformaldehyde for 20 min, washed with PBS, and incubated with crystal violet for 20 min. Finally, cells were washed, a solution of sodium dodecyl sulfate (1%) was added for 1 h, and the absorbance at 595 nm was quantified. The fluorescence intensity was normalized to the absorbance at 595 nm and related to the control value.

hGF Live/Dead Cell Count and Cell Cycle Analyses. For cell live/dead cell count hGF were seeded in a six-well microplate (80 000 cells/well) and were treated in complete medium with compound **6** (1–5 μM) in the absence or in the presence of H_2O_2 (200 μM) for 72 h. The number of live cells and the percentage of dead cells were quantified and analyzed by Muse Cell Analyzer (Merck KGaA, Darmstadt, Germany), according to the manufacturer's instructions (MCH100102 Muse Count & Viability assay kit, Merck Millipore). For the cell cycle analysis, hGF were seeded and treated as above. The quantification of the percentage of cells in the different cell phases was performed using the Muse Cell Analyzer (MCH100106 Muse cell cycle assay kit, Merck Millipore) as previously reported.[49]

Real-Time RT-PCR Analysis. The gene expression in hGF was quantified by performing a real-time RT-PCR analysis. Briefly, hGF (3500 cells/cm^2) were treated in complete medium with compound **6** (1–5 μM) in the absence or in the presence of H_2O_2 (200 μM) or LPS (1 μg/mL) for 72 h. The cells were collected, and the total RNA was extracted using the Rneasy mini kit (Qiagen, Hilden, Germany) according to the manufacturer's instructions. The purity of the RNA samples was determined by measuring the absorbance at 260/280 nm. mRNA (500 ng) was retrotranscribed to single-strand cDNA using the i-Script cDNA synthesis kit (BioRad) following the manufacturer's instructions. Real-time RT-PCR reactions were performed with Fluocycle II SYBR in the presence of 50 ng of cDNA and 200 nM forward and reverse primers.[48,50] The primers were designed to span intron/exon boundaries to exclude genomic DNA impurity, and β-actin was used as the housekeeping gene. p53 FOR: 5′-CTTTGAGGTGCGTGTTTGTG-3′ REV: 5′-GTGGTTTCTTCTTTGGCTGG-3′ (161 bp); p21 FOR: 5′-TGCCGAAGTCAGTTCCTTG-3′ REV: 5′-CATGGGTTCTGACGGACATC-3′ (134 bp); $p16^{INK4A}$ (CDKN2A) FOR: 5′-GACCCCGCCACTCTCACC-3′ REV: 5′-CCTGTAGGACCTTCGGTGACTGA-3′ (318 bp); IL-6 FOR: 5′-TCCTCGACGGCATCTCA-3′ REV: 5′-TTTTCACCAGGCAAGTCTCCT-3′ (165 bp); IL-8 FOR: 5′-AAGAGAGCTCTGTCTGGACC-3′ REV: 5′-GATATTCTCTTGGCCCTTGG-3′ (408 bp); IL-10 FOR: 5′-CAAGCTGAGAACCAAGACCC-3′ REV: 5′-AAGATGTCAAACTCACTCATGGC-3′ (141 bp); β-actin FOR: 5′-GCACTCTTCCAGCCTTCCTTCC-3′ REV: 5′-GAGCCGCCGATCCACACG-3′ (254 bp). All reactions were performed for 40 cycles using the following temperature profiles: 98 °C for 30 s; 57 °C for 20 s; and 72 °C for 30 s. The mRNA levels were normalized with

https://dx.doi.org/10.1021/acs.jnatprod.9b01030
J. Nat. Prod. 2020, 83, 626–637

β-actin mRNA levels, and the relative expression was calculated using the Ct value. PCR specificity was determined by both melting curve analysis and gel electrophoresis.

Statistical Analysis. Data were analyzed with GraphPad Prism program (GraphPad Software Inc., San Diego, CA, USA). All data are represented as the mean ± SD. Statistical analysis was performed as indicated in figure legends. A p-value of <0.05 was considered to be statistically significant.

■ ASSOCIATED CONTENT

Supporting Information

The Supporting Information is available free of charge at https://pubs.acs.org/doi/10.1021/acs.jnatprod.9b01030.

NMR spectra of compounds **1**−**5** (PDF)

■ AUTHOR INFORMATION

Corresponding Author

Nunziatina De Tommasi − *Dipartimento di Farmacia, Università degli Studi di Salerno, 84084 Fisciano, SA, Italy;* orcid.org/0000-0003-1707-4156; Phone: +39-089-969754; Email: detommasi@unisa.it; Fax: +39-089-969602

Authors

Anna Maria Iannuzzi − *Dipartimento di Farmacia, Università di Pisa, 56126 Pisa, Italy*

Chiara Giacomelli − *Dipartimento di Farmacia and Centro Interdipartimentale di Ricerca "Nutraceutica e Alimentazione per la Salute", Università di Pisa, 56126 Pisa, Italy;* orcid.org/0000-0002-6244-602X

Marinella De Leo − *Dipartimento di Farmacia and Centro Interdipartimentale di Ricerca "Nutraceutica e Alimentazione per la Salute", Università di Pisa, 56126 Pisa, Italy;* orcid.org/0000-0002-5544-8457

Deborah Pietrobono − *Dipartimento di Farmacia, Università di Pisa, 56126 Pisa, Italy;* orcid.org/0000-0002-4986-1472

Fabiano Camangi − *Scuola Superiore Sant'Anna di Studi Universitari e di Perfezionamento, 56127 Pisa, Italy*

Claudia Martini − *Dipartimento di Farmacia and Centro Interdipartimentale di Ricerca "Nutraceutica e Alimentazione per la Salute", Università di Pisa, 56126 Pisa, Italy;* orcid.org/0000-0001-9379-3027

Maria Letizia Trincavelli − *Dipartimento di Farmacia and Centro Interdipartimentale di Ricerca "Nutraceutica e Alimentazione per la Salute", Università di Pisa, 56126 Pisa, Italy;* orcid.org/0000-0001-8124-977X

Alessandra Braca − *Dipartimento di Farmacia and Centro Interdipartimentale di Ricerca "Nutraceutica e Alimentazione per la Salute", Università di Pisa, 56126 Pisa, Italy;* orcid.org/0000-0002-9838-0448

Complete contact information is available at: https://pubs.acs.org/10.1021/acs.jnatprod.9b01030

Notes

The authors declare no competing financial interest.

■ ACKNOWLEDGMENTS

This work was financially supported by Fondi di Ateneo PRA_2017_30, University of Pisa, and FARB 2018, University of Salerno. We also thank Dr. Lara Russo for her expert technical assistance.

■ DEDICATION

Dedicated to Dr. Jon Clardy of Harvard Medical School for his pioneering work on bioactive natural products.

■ REFERENCES

(1) Liao, C. R.; Ho, Y. L.; Huang, G. J.; Yang, C.; Chao, C. Y.; Chang, Y. S.; Kuo, Y. H. *Molecules* **2013**, *18*, 13218−13227.

(2) Ozen, T.; Yenigun, S.; Altun, M.; Demirtas, I. *Comb. Chem. High Throughput Screening* **2017**, *20*, 559−578.

(3) Sabir, M. S.; Ahmad, D. S.; Hussain, I. M.; Hon, M.; Tahir, K. M. *Saudi Med. J.* **2007**, *28*, 259−263.

(4) Ito, H.; Miki, K.; Yoshida, T. *Chem. Pharm. Bull.* **1999**, *47*, 536−542.

(5) Ishaq, S.; Rathore, H. A.; Sabir, S. M.; Maroof, M. S. *Food Sci. Biotechnol.* **2015**, *24*, 673−679.

(6) Pei, R.; Yu, M.; Bruno, R.; Bolling, B. W. *J. Funct. Foods* **2015**, *16*, 305−314.

(7) Galasso, G.; Conti, F.; Peruzzi, L.; Ardenghi, N. M. G.; Banfi, E.; Celesti-Grapow, L.; Albano, A.; Alessandrini, A.; Bacchetta, G.; Ballelli, S.; Bandini Mazzanti, M.; Barberis, G.; Bernardo, L.; Blasi, C.; Bouvet, D.; Bovio, M.; Cecchi, L.; Del Guacchio, E.; Domina, G.; Fascetti, S.; Gallo, L.; Gubellini, L.; Guiggi, A.; Iamonico, D.; Iberite, M.; Jiménez-Mejías, P.; Lattanzi, E.; Marchetti, D.; Martinetto, E.; Masin, R. R.; Medagli, P.; Passalacqua, N. G.; Peccenini, S.; Pennesi, R.; Pierini, B.; Podda, L.; Poldini, L.; Prosser, F.; Raimondo, F. M.; Roma-Marzio, F.; Rosati, L.; Santangelo, A.; Scoppola, A.; Scortegagna, S.; Selvaggi, A.; Selvi, F.; Soldano, A.; Stinca, A.; Wagensommer, R. P.; Wilhalm, T.; Bartolucci, F. *Plant Biosystems* **2018**, *152*, 556−592.

(8) Spínola, V.; Pinto, J.; Llorent-Martínez, E. J.; Castilho, P. C. *Food Res. Int.* **2019**, *122*, 283−294.

(9) Olszowy, M. *Plant Physiol. Biochem.* **2019**, *144*, 135−143.

(10) Wang, J.; Fang, X.; Ge, L.; Cao, F.; Zhao, L.; Wang, Z.; Xiao, W. *PLoS One* **2018**, *13*, No. e0197563.

(11) Xiao, J. *Crit. Rev. Food Sci. Nutr.* **2017**, *57*, 1874−1905.

(12) Wang, Y.; Andrukhov, O.; Rausch-Fan, X. *Front. Physiol.* **2017**, *8*, 910.

(13) Sonis, S. T.; Fey, E. G. *Oncology (Williston Park)* **2002**, *16*, 680−695.

(14) Chapple, I. L. *J. Clin. Periodontol.* **1997**, *24*, 287−296.

(15) Ling, M. R.; Chapple, I. L.; Matthews, J. B. *J. Clin. Periodontol.* **2016**, *43*, 652−658.

(16) Bae, W. J.; Park, J. S.; Kang, S. K.; Kwon, I. K.; Kim, E. C. *Int. J. Mol. Sci.* **2018**, *19* (pii), E1742.

(17) Yoshino, F.; Yoshida, A.; Nakajima, A.; Wada-Takahashi, S.; Takahashi, S. S.; Lee, M. C. *PLoS One* **2013**, *8*, No. e82834.

(18) Ramesh, A.; Varghese, S. S.; Doraiswamy, J. N.; Malaiappan, S. *J. Intercult. Ethnopharmacol.* **2016**, *5*, 92−96.

(19) Zhang, Q. Y.; Wang, F. X.; Jia, K. K.; Kong, L. D. *Front. Pharmacol.* **2018**, *9*, 1253.

(20) Giacomelli, C.; Natali, L.; Nisi, M.; De Leo, M.; Daniele, S.; Costa, B.; Graziani, F.; Gabriele, M.; Braca, A.; Trincavelli, M. L.; Martini, C. *Stem Cell Res. Ther.* **2018**, *9*, 135.

(21) Koohi-Hosseinabadi, O.; Ranjbar, Z.; Sepehrimanesh, M.; AndisheTadbir, A.; Poorbaghi, Sl L.; Bahranifard, H.; Tanideh, N.; Koohi-Hosseinabadi, M.; Irajiet, A. *Environ. Sci. Pollut. Res.* **2017**, *24*, 24447−24453.

(22) Sang, S.; Cheng, X.; Fu, H.-Y.; Shieh, D.-E.; Bai, N.; Lapsley, K.; Stark, R. E.; Rosen, R. T.; Ho, C.-T. *Tetrahedron Lett.* **2002**, *43*, 2547−2549.

(23) Kim, S. Y.; Koo, Y. K.; Koo, J. K.; Ngoc, T. M.; Kang, S. S.; Bae, K. H.; Kim, Y. S.; Yun-Choi, H. S. *J. Med. Food* **2010**, *13*, 1069−1074.

(24) Kite, G. C.; Veitch, N. C.; Boalch, M. E.; Lewis, G. P.; Leon, C. J.; Simmonds, N. S. J. *Phytochemistry* **2009**, *70*, 785−794.

(25) Kim, H. K.; Jeon, W. K.; Ko, B. S. *Nat. Prod. Sci.* **2000**, *6*, 79−81.

(26) Pauli, G. F.; Junior, P. *Phytochemistry* **1995**, *38*, 1245−1250.

(27) Markham, K. R.; Hammett, K. R. W.; Ofman, D. J. *Phytochemistry* **1992**, *31*, 549−554.
(28) Leitao, G. C.; Soares, S. S. V.; de Barros, T.; Brito, M.; DelleMonache, F. *Phytochemistry* **2000**, *55*, 679−682.
(29) Agrawal, P. K. *Carbon-13 NMR of Flavonoids*; Elsevier: Amsterdam, 1989; pp 334−335.
(30) Iwaoka, E.; Oku, H.; Takahashi, Y.; Ishiguro, K. *Biol. Pharm. Bull.* **2009**, *32*, 509−512.
(31) Liu, C. D.; Chen, J.; Wang, J. H. *Chem. Nat. Compd.* **2009**, *45*, 808−810.
(32) Paudel, S. B.; Park, J.; Kim, N. H.; Choi, H.; Seo, E.-K.; Woo, H. A.; Nam, J.-W. *Fitoterapia* **2019**, *139*, 104374.
(33) Kiyoshima, T.; Enoki, N.; Kobayashi, I.; Sakai, T.; Nagata, K.; Wada, H.; Fujiwara, H.; Ookuma, Y.; Sakai, H. *Int. J. Mol. Med.* **2012**, *30*, 1007−1012.
(34) Spagnuolo, G.; D'Antò, V.; Cosentino, C.; Schmalz, G.; Schweikl, H.; Rengo, S. *Biomaterials* **2006**, *27*, 1803−1809.
(35) Davalli, P.; Mitic, T.; Caporali, A.; Lauriola, A.; D'Arca, D. *Oxid. Med. Cell. Longevity* **2016**, *2016*, 3565127.
(36) Papież, M. A.; Krzyściak, W. *ActaBiochim. Polym.* **2014**, *61*, 795−799.
(37) Yan, L. J. *Redox Biol.* **2014**, *2*, 165−169.
(38) Lionetti, M. C.; Mutti, F.; Soldati, E.; Fumagalli, M. R.; Coccé, V.; Colombo, G.; Astori, E.; Miani, A.; Milzani, A.; Dalle-Donne, I.; Ciusani, E.; Costantini, G.; La Porta, C. A. M. *Int. J. Environ. Res. Public Health* **2019**, *16* (pii), E657.
(39) Santa-Gonzalez, G. A.; Gomez-Molina, A.; Arcos-Burgos, M.; Meyer, J. N.; Camargo, M. *Redox Biol.* **2016**, *9*, 124−133.
(40) Chandrasekaran, A.; Idelchik, M. D. P. S.; Melendez, J. A. *Redox Biol.* **2017**, *11*, 91−102.
(41) Imatani, T.; Kato, T.; Okuda, K. *Oral Microbiol. Immunol.* **2001**, *16*, 65−72.
(42) Kim, B.-R.; Kim, H. Y.; Choi, I.; Kim, J.-B.; Jin, C. H.; Han, A.-R. *Molecules* **2018**, *23* (pii), E1998.
(43) Kluska, M.; Juszczak, M.; Wysokiński, D.; Żuchowski, J.; Stochmal, A.; Woźniak, K. *Toxicol. Res.* **2019**, *8*, 896−907.
(44) Fang, Y.; Cao, W.; Xia, M.; Pan, S.; Xu, X. *Nutrients* **2017**, *9* (pii), 1301.
(45) Tarahovsky, Y. S.; Kim, Y. A.; Yagolnik, E. A.; Muzafarov, E. N. *Biochim. Biophys. Acta, Biomembr.* **2014**, *1838*, 1235−1246.
(46) Dal Piaz, F.; Vera Saltos, M. B.; Franceschelli, S.; Forte, G.; Marzocco, S.; Tuccinardi, T.; Poli, G.; Ebrahimi, S. N.; Hamburger, M.; De Tommasi, N.; Braca, A. *J. Nat. Prod.* **2016**, *79*, 2681−2692.
(47) Braca, A.; Sinisgalli, C.; De Leo, M.; Muscatello, B.; Cioni, P. L.; Milella, L.; Ostuni, A.; Giani, S.; Sanogo, R. *Molecules* **2018**, *23* (pii), E3104.
(48) Da Pozzo, E.; Tremolanti, C.; Costa, B.; Giacomelli, C.; Milenkovic, V. M.; Bader, S.; Wetzel, C. H.; Rupprecht, R.; Taliani, S.; Da Settimo, F.; Martini, C. *Int. J. Mol. Sci.* **2019**, *20* (pii), E4467.
(49) Giacomelli, C.; Daniele, S.; Natali, L.; Iofrida, C.; Flamini, G.; Braca, A.; Trincavelli, M. L.; Martini, C. *Sci. Rep.* **2017**, *7*, 15174.
(50) Giacomelli, C.; Natali, L.; Trincavelli, M. L.; Daniele, S.; Bertoli, A.; Flamini, G.; Braca, A.; Martini, C. *Int. J. Biochem. Cell Biol.* **2016**, *74*, 95−108.

https://dx.doi.org/10.1021/acs.jnatprod.9b01030
J. Nat. Prod. 2020, 83, 626−637